Supplementary material

Templated synthesis of multi-hierarchical layered double hydroxide microspheres

Tomasz Kondratowicz,[a] Cyril Besnard[b], Zoe Turner[a], Jin-Chong Tan[b], Chunping Chen[a]*, Roland Turnell-Ritson, and Dermot O'Hare[a]*

[a] Chemistry Research Laboratory, Department of Chemistry, University of Oxford, 12 Mansfield Road, Oxford, OX1 3TA, UK. E-mail: chunping.chen@chem.ox.ac.uk; dermot.ohare@chem.ox.ac.uk; Tel: +44(0)1865 272686

[b] Department of Engineering Science, University of Oxford, Parks Road, Oxford, OX1 3PJ, UK

Contents

1. Experimental section
2. Supporting figures
3. Supporting tables

Experimental section

Synthesis

Al recycling study

After the primary synthesis, the filtrate was collected in a filter flask and then poured into the same Teflon-lined stainless-steel autoclave together with a new portion of MgO matrix (100 mg). Then, after

4 h of reaction at 80 C, the solid sample was filtered and the filtrate was collected and reused. Four successive cycles were performed in this way.

Characterization

Crystallographic structure of samples was determined by Bruker D8 diffractometer with CuKα radiation (λ_1 = 1.544 Å and λ_2 = 1.541 Å) operated at 40 kV and 30mA. Solid samples were mounted on PMMA sample holders and XRD patterns were recorded in the range of 2θ = 5-70° with a step of 0.01°. The LDH lattice parameters *a* and *c* were calculated from the diffraction plane positions of (110) and (003), respectively ($a = 2d_{110}$, $c = 3d_{003}$). Crystallite size of LDH in stacking or plane direction ($D_{(003)}$ and $D_{(110)}$, respectively), calculated according to Scherrer equation: $D_{(hkl)}=0.9\cdot\lambda/(\beta\cdot\cos\theta)$, λ=0.154 nm, θ is the Bragg diffraction angle (deg.), and β is the FWHM (rad.) of the diffraction peaks.

Nitrogen adsorption-desorption isotherms were recorded at -196 °C using a Micromeritics TriStar II instrument. Before the measurements, samples were degassed overnight under vacuum at 130 °C. Total pore volumes (V_{total}) were obtained from amounts of nitrogen adsorbed at relative pressure of 0.99, while the specific surface areas (S_{BET}) were determined by the BET method.

Inductively coupled plasma optical emission spectroscopy (ICP-OES) analyses were carried out at Department of Chemistry, University of Cambridge. Measurements were performed on a Themo Fisher Scientific iCAP 7400 Duo ICP Spectrometer. Calibration was performed by construction of a standard curve using ICP standards from Sigma-Aldrich. Samples were run in ∼2 % nitric acid (Fisher TraceMetal grade). Samples were weighed on a Mettler UMT2 balance and dissolved in 5 mL nitric acid, diluted with 5 mL water and a 0.5 mL aliquot was diluted to 10 mL with water.

Elemental analysis was performed using a ThermoFlash 2000 (Thermo Scientific) CHN analyser at London Metropolitan University.

Thermogravimetric analyses (TGA) were performed using a PerkinElmer TGA 8000. A sample of approximately 10 mg was heated under a nitrogen atmosphere (20 $mL\cdot min^{-1}$) from 30 to 800 °C at a heating rate of 2 $°C\cdot min^{-1}$.

FT-IR spectra were measured on a Bruker Vertex 80 spectrometer fitted with a DuraSamplIR Diamond ATR accessory. 256 background scans were taken before 128 sample scans were recorded on sample powder, capturing the transmittance signals between 400-4000 cm^{-1} at a 2 cm^{-1} resolution.

Temperature-programmed desorption of carbon dioxide (TPD-CO_2) was performed using a Micromeritics AutoChem II 2920 equipped with a TCD detector. 100 mg of a calcined sample was outgassed in a flow of helium (20 mL/min) at 450 °C for 1 h, and then cooled down to 25 °C. The CO_2 uptake from a stream of CO_2 with a flow rate of 50 $°C\cdot min^{-1}$ for 1 h. Weakly adsorbed CO_2 was removed by flushing with He at 25 °C for 1 h. The desorption of CO_2 was analyzed in the temperature range of 25–450 °C at the heating rate of 10 $°C\cdot min^{-1}$.

SEM Tescan Lyra 3 (Tescan, Czech Republic) was used to acquired secondary and backscattered electron images using an accelerating voltage of 5 keV. For the internal details of the particles, a focused ion beam with the gallium (Ga) source was used at 30 kV with an emission current of 2 μA, at the angle of incidence 55° between the FIB and electron beam. Slice and view using 3D wizard implemented in Lyra software was used [1], with makers milled using a probe current of 1.6 nA to account for drift during the FIB milling. Then the slicing was setup with pixel size of 30 nm and slice thickness of 141 nm for the two samples and milling done with a probe current of 1.6 nA. Secondary and backscattered electron images were then simultaneously acquired during the process. A foreshortening correction[2] was carried out in Lyra software with the dynamic and tilt rotation enabled to compensate for the tilt stage during the acquisition of the images. Energy-dispersive X-ray spectroscopy (EDX) elemental analysis in the SEM was carried using X-Max 150 EDS detector (Oxford Instruments, U.K) at 5 keV. Maps were acquired and interpreted using Aztec Oxford Instruments software.

A scanning electron microscope (Jeol JSM 6010) was used to study the low-resolution surface morphology using an accelerating voltage of 10–20 kV. Samples were prepared before imaging by dispersing powder onto a carbon spot and coated with platinum using a Quorum SC7620 Sputter Coater for 120 s.

CO_2 capture measurement

Before each measurement, the samples were calcined in a crucible at 450 °C for 3 h (heating rate 5 °C·min^{-1}) in a muffle furnace to convert them into stable oxide systems. Then, approximately 150 mg of the sample was placed in a quartz tube and degassed overnight in a vacuum at 130 °C. The tube with the sample was then mounted in the Micromeritics 3Flex instrument and degassed again at 120 °C for 1 h. After cooling to 40 °C, the sample was allowed to evacuate in a vacuum for 10 min. CO_2 measurements were then taken at 40 °C and the maximum value read was the total adsorption.

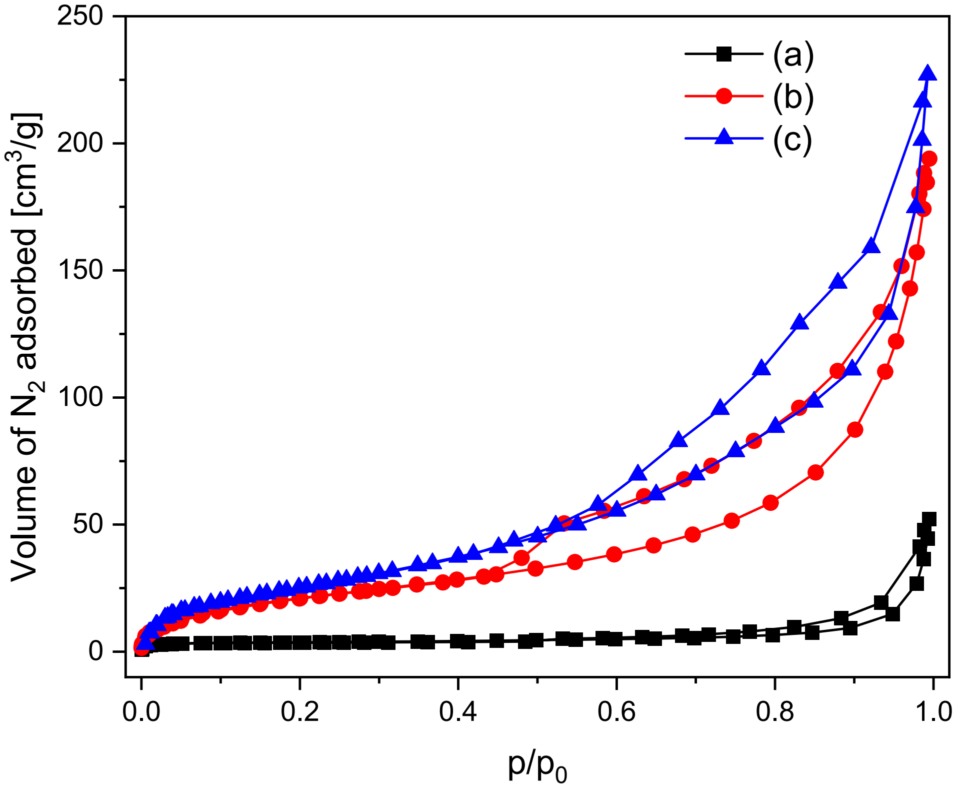

Fig. S1. N_2 adsorption-desorption isotherms (a)MgO(p), (b) MgO and (c) MgAl(4h_0.2).

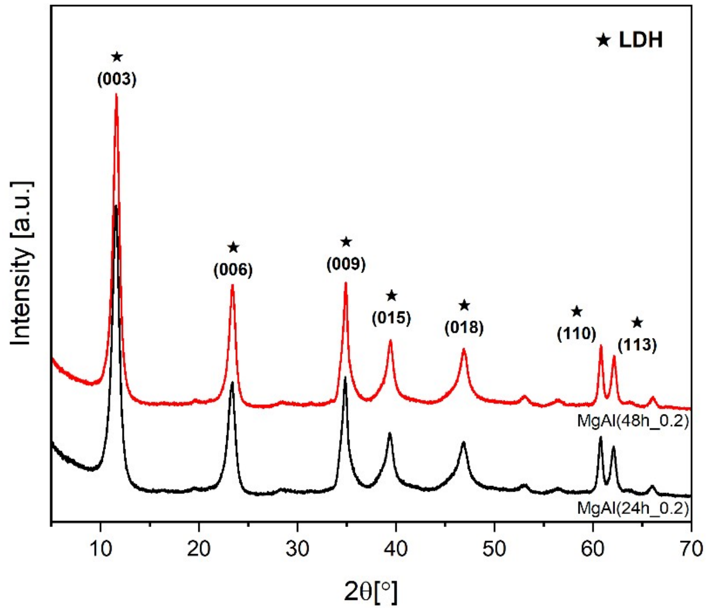

Fig. S2. XRD patterns of MgO after 24 and 48 h of hydrothermal modification (all reflections were indexed as Mg/Al LDH PDF No. 01-070-2151).

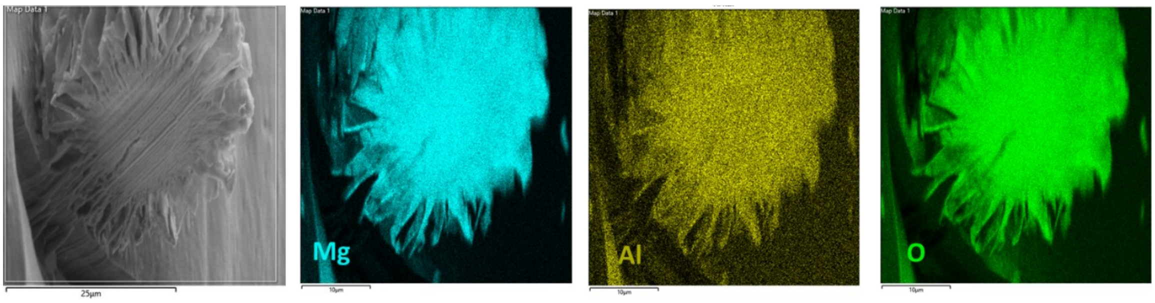

Fig. S3. EDX mapping of cross-sectional MgAl(15min_0.2) microspheres.

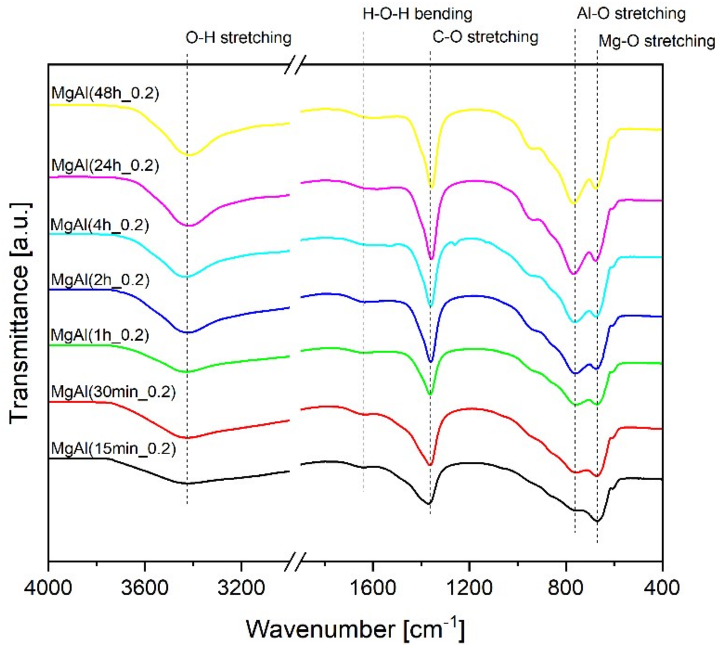

Fig. S4. FT-IR spectra of the MgO after different time of hydrothermal modification.

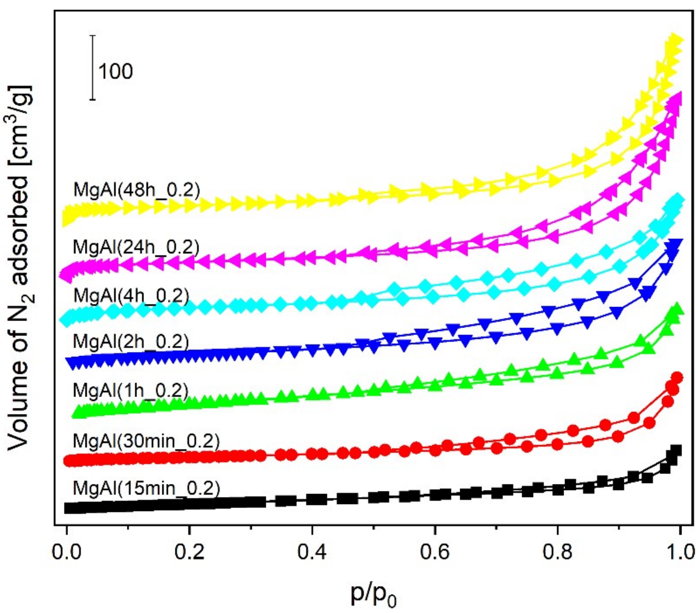

Fig. S5. N_2 adsorption-desorption isotherms of the MgO after different time of hydrothermal modification.

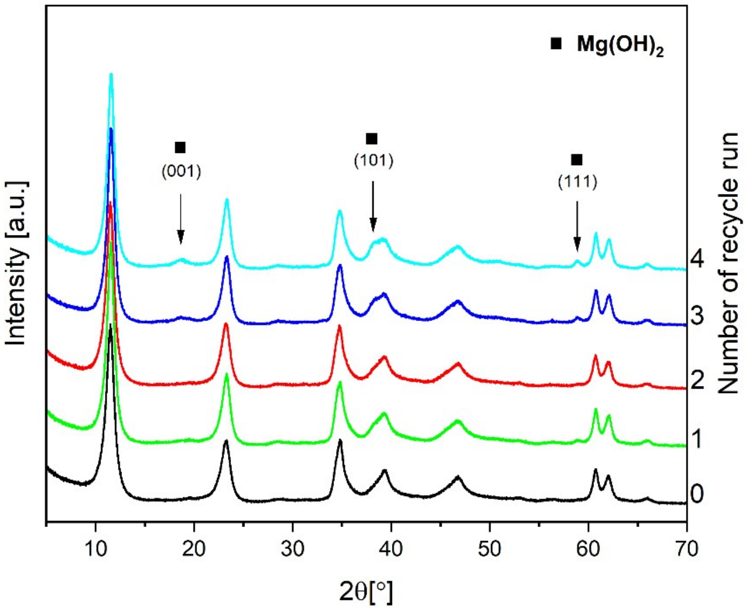

Fig. S6. XRD patterns after the virgin synthesis (recycle run = 0) and four subsequent synthesis iterations with the recovered spent Al-containing solution (recycle run = 1–4), the reflections of impurity phase were indexed as $Mg(OH)_2$ PDF No. 01-083-0144.

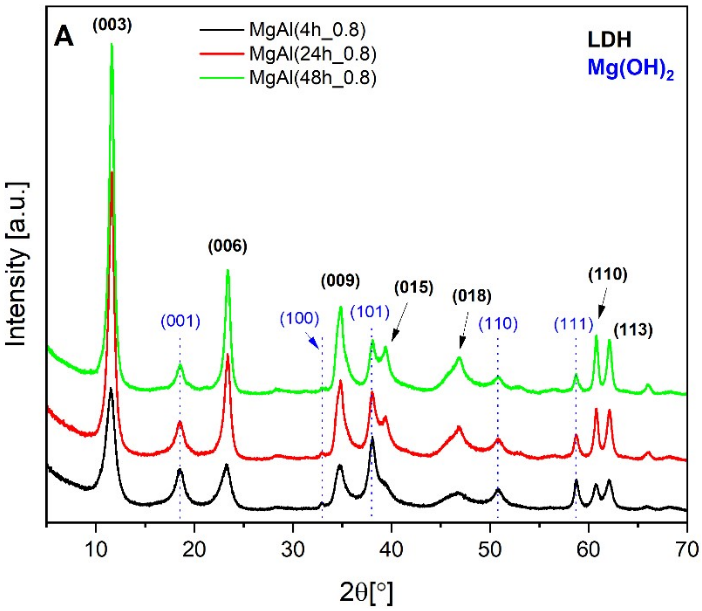

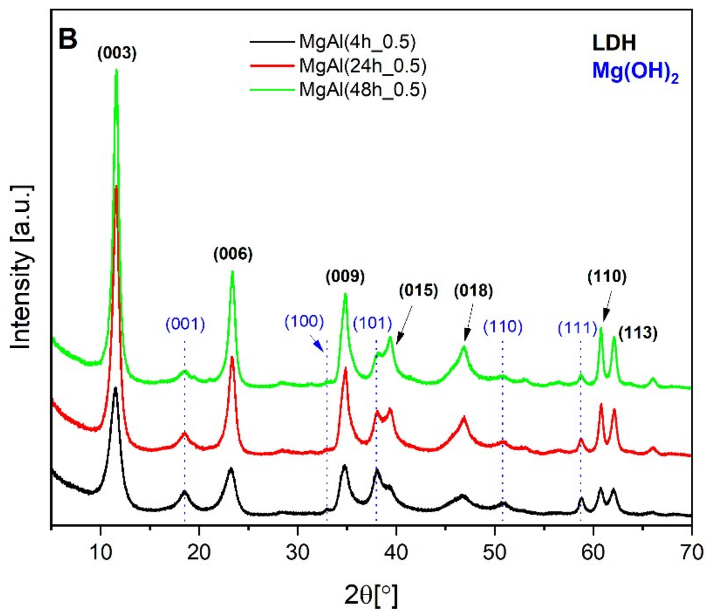

Fig. S7. XRD patterns of the samples synthesised at different time of hydrothermal modification with 0.09 M (A) and 0.14 M (B) $NaAlO_2$ solution (Mg/Al input = 0.8 and 0.5, respectively).

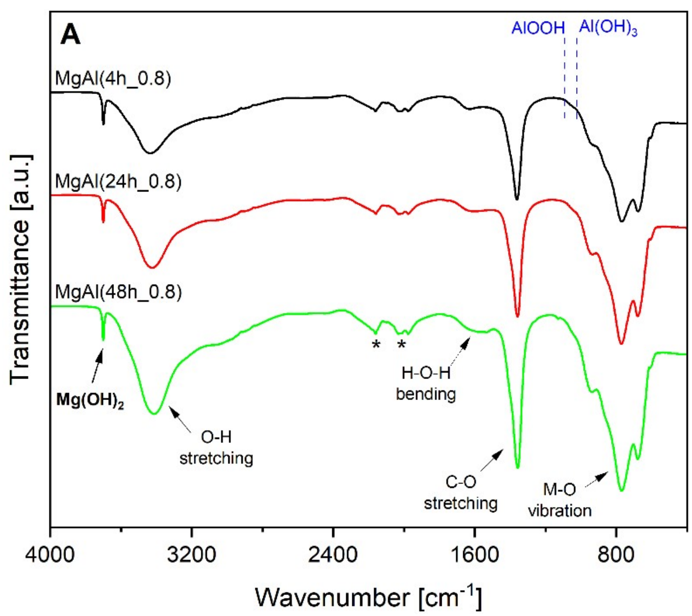

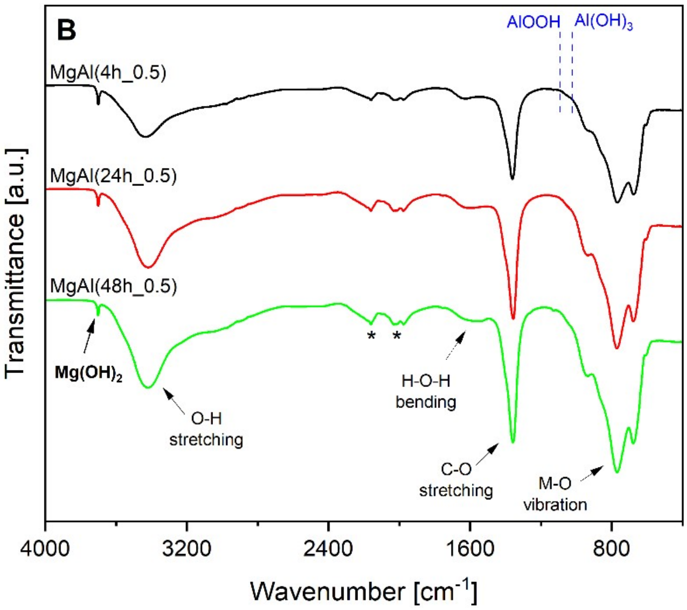

Figure S8. FT-IR spectra of the samples synthesised at different time of hydrothermal modification with 0.09 M (A) and 0.14 M (B) $NaAlO_2$ solution (Mg/Al input = 0.8 and 0.5, respectively).

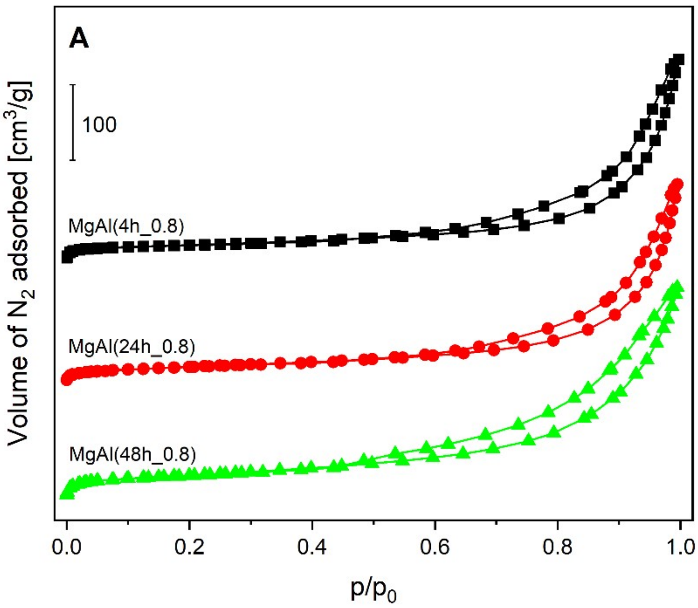

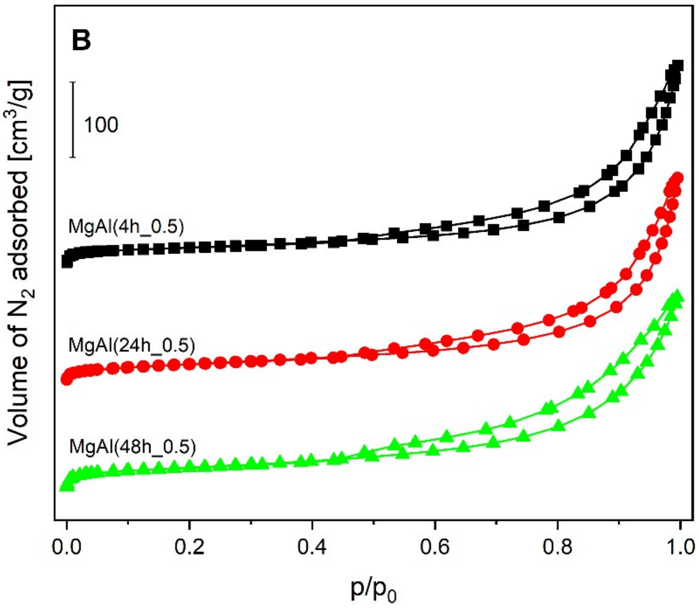

Fig. S9. N_2 adsorption-desorption isotherms of the samples obtained at different time of hydrothermal modification with 0.09 M (A) and 0.14 M (B) $NaAlO_2$ solution (Mg/Al input = 0.8 and 0.5, respectively).

Supporting tables

Table S0. Comparison with other materials

Sample	S_{BET} [$m^2 \cdot g^{-1}$]	V_{total} [$cm^3 \cdot g^{-1}$]	Adsorption Temperature [°C]	CO2 Adsorption [$mmol \cdot g^{-1}$]		
MgAl(48h_0.8)					110	0.44

[1] Determined by ICP-OES
[2] Determined by XRD calibration curve[3]

Table S1. Element analysis for selected samples.

Sample	Mg[1] [wt.%]	Al[1] [wt.%]	C[2] [wt.%]	H[2] [wt.%]	N[2] [wt.%]
MgO(P)	24.39	-	9.87	2.40	0.00
MgO	55.94	-	1.28	0.15	0.00
MgAl(4h_0.2)	17.67	12.04	3.74	3.23	0.00

[1] Obtained from ICP-OES
[2] Obtained from CHN analysis

Table S2. Textural properties of the selected samples.

Sample	S_{BET} [$m^2 \cdot g^{-1}$]	V_{total} [$cm^3 \cdot g^{-1}$]
MgO(P)	14	0.08
MgO	101	0.34
MgO(commercial)	26	0.10
MgAl(4h_0.2)	84	0.30

Table S3. Crystal properties of the MgO after hydrothermal modification at different time.

Sample	LDH lattice parameters[1] [nm]		LDH basal spacing [nm]	Crystallite size[2] [nm]	
	a	c	d	$D_{(003)}$	$D_{(110)}$
MgAl(15min_0.2)	0.303	2.329	0.776	4.1	4.6
MgAl(30min_0.2)	0.304	2.325	0.775	4.9	6.2
MgAl(1h_0.2)	0.305	2.321	0.774	6.1	10.0
MgAl(2h_0.2)	0.305	2.319	0.773	6.9	13.2
MgAl(4h_0.2)	0.305	2.310	0.770	7.4	14.9
MgAl(24h_0.2)	0.305	2.301	0.767	9.8	22.0
MgAl(48h_0.2)	0.305	2.290	0.763	10.8	23.1

[1] $a = 2d_{110}$, $c = 3d_{003}$

[2] Crystallite size of LDH in stacking or plane direction ($D_{(003)}$ and $D_{(110)}$, respectively), calculated according to Scherrer equation: $D_{(hkl)}=0.9\cdot\lambda/(\beta\cdot\cos\theta)$, $\lambda=0.154$ nm, θ is the Bragg diffraction angle (deg.), and β is the FWHM (rad.) of the diffraction peaks.

Table S4. Composition and textural properties of the MgO after hydrothermal modification at different time.

Sample	Mg[1] [wt.%]	Al[1] [wt.%]	Molar Mg/Al[1]	Molar Mg/Al[2]	S_{BET} $[m^2\cdot g^{-1}]$	V_{total} $[cm^3\cdot g^{-1}]$
MgAl(15min_0.2)	33.30	5.32	6.95	1.37	34	0.15
MgAl(30min_0.2)	27.10	7.63	3.94	1.72	45	0.21
MgAl(1h_0.2)	22.10	10.04	2.44	2.32	78	0.27
MgAl(2h_0.2)	18.40	11.58	1.76	2.38	82	0.31
MgAl(4h_0.2)	17.67	12.04	1.63	2.34	84	0.30
MgAl(24h_0.2)	17.43	12.20	1.59	2.30	92	0.44
MgAl(48h_0.2)	18.90	11.76	1.78	2.19	97	0.45

[1] Determined by ICP-OES

[2] Determined by XRD calibration curve

Table S5. Crystal properties of the MgO after hydrothermal modification at different time (Mg/Al input = 0.5 and 0.8).

Sample	LDH lattice parameters[1] [nm]		LDH basal spacing [nm]	Crystallite size[2] [nm]	
	a	c	d	$D_{(003)}$	$D_{(110)}$
MgAl(4h_0.5)	0.305	2.315	0.772	7.1	13.8
MgAl(24h_0.5)	0.305	2.297	0.766	10.7	20.4
MgAl(48h_0.5)	0.305	2.294	0.765	12.5	23.5
MgAl(4h_0.8)	0.305	2.309	0.770	7.7	14.1
MgAl(24h_0.8)	0.305	2.292	0.764	12.4	21.8
MgAl(48h_0.8)	0.305	2.287	0.762	14.3	24.2

[1] $a = 2d_{110}$, $c = 3d_{003}$

[2] Crystallite size of LDH in stacking or plane direction ($D_{(003)}$ and $D_{(110)}$, respectively), calculated according to Scherrer equation: $D_{(hkl)}=0.9 \cdot \lambda/(\beta \cdot \cos\theta)$, λ=0.154 nm, θ is the Bragg diffraction angle (deg.), and β is the FWHM (rad.) of the diffraction peaks.

Table S6. Composition and textural properties of the MgO after hydrothermal modification at different time (Mg/Al input = 0.5 and 0.8).

Sample	Mg[1] [wt.%]	Al[1] [wt.%]	Molar Mg/Al[1]	Molar Mg/Al[2]	S_{BET} [$m^2 \cdot g^{-1}$]	V_{total} [$cm^3 \cdot g^{-1}$]
MgAl(4h_0.5)	21.98	8.48	2.88	2.38	82	0.42
MgAl(24h_0.5)	18.88	9.33	2.25	2.27	92	0.43
MgAl(48h_0.5)	21.40	11.06	2.15	2.29	103	0.41
MgAl(4h_0.8)	22.39	7.21	3.45	2.34	72	0.42
MgAl(24h_0.8)	20.28	8.57	2.63	2.26	80	0.42
MgAl(48h_0.8)	22.80	10.49	2.41	2.24	110	0.44

[1] Determined by ICP-OES

[2] Determined by XRD calibration curve[3]

1. C. Besnard, A. Marie, P. Buček, S. Sasidharan, R. A. Harper, S. Marathe, K. Wanelik, G. Landini, R. M. Shelton and A. M. Korsunsky, *Materials & Design*, 2022, **220**, 110829.
2. J. D. Arregui-Mena, P. D. Edmondson, A. A. Campbell and Y. Katoh, *Journal of Nuclear Materials*, 2018, **511**, 164-173.
3. P. Kenyon, S. Roberts, Z. R. Turner, N. H. Rees and D. O'Hare, *The Journal of Physical Chemistry C*, 2024, **128**, 12249-12258.